EUROPEAN ORGANIZATION FOR NUCLEAR RESEARCH
ORGANISATION EUROPEENNE POUR LA RECHERCHE NUCLEAIRE

CERN - PS DIVISION

PS/ BD/ Note 94-04

PROFILOMETER FOR SMALL DIMENSION PROTON BEAMS

J. BOSSER, I. MESHKOV*

*) Joint Institute for Nuclear Research (JINR) - Dubna.

Geneva, Switzerland
7 March, 1994

1. INTRODUCTION

The advent of accelerators like the LHC, using small transverse dimension beams has motivated the investigation (or rejuvenation) and studies of new methods aimed at measuring beams whose diameters are less than 1 mm, with good resolution. Some of these methods make use of thin, charged or neutral, beams crossing the beam to be sensed (Refs. 1 and 2).

In the present paper we intend to study the feasibility of some of the above methods and techniques, in order to measure the transverse distribution of proton beams foreseen for the LHC.

After introducing some definitions and parameters we shall study how positive or neutral pencil beams could be used for our purpose.

Examples (or numerical application: N.A) will be taken using the very dense bunched LHC beam (Cases 1 and 2) or the low-density-coasting LEAR beam (Case 4). Case 3, which concerns the PS, is a simple extrapolation of Case 1.

2. DATA, PARAMETERS

2.1 Symbols

q: Elementary charge, $q = 1.6 \cdot 10^{-19}$ [C]
ε_0: Vacuum permittivity, $\varepsilon_0 = 8.854 \cdot 10^{-12}$ [F·m^{-1}], $1/4 \cdot \pi \cdot \varepsilon_0 = 8.987 \cdot 10^{9}$[F^{-1}·m]
μ_0: Vacuum permeability, $\mu_0 = 4 \cdot \pi \cdot 10^{-7}$[H·m^{-1}]
r[m] radius, x[m] horizontal coordinate, z[m] vertical coordinate (see Fig. 1)
s[m] longitudinal coordinate. Elementary volume $dv = r \cdot dr \cdot d\phi \cdot ds$
m_p: Proton mass, $m_p = 1.672 \cdot 10^{-27}$[kg]
$\beta = v/c$, $\gamma = (1 - \beta^2)^{-1/2}$, where v is the velocity and $c = 3 \cdot 10^8$ [m·s^{-1}].

2.2 Parameters of the LHC proton beam

	Case 1	Case 2
Proton energy [TeV]	0.45	8
Gaussian rms radius Δ_r [mm]	1 (a)	0.25 (a)
rms bunch length Δ_s [cm]	7.5	7.5
Distance between bunches [m]	7.5	7.5
Number of particles per bunch: n_b	$1.6\ 10^{11}$	$1.6\ 10^{11}$
Number of bunches: n_0	2835	2835
Revolution frequency: fr [Hz]	11245.51	11245.51
Average beam current [A]	0.85	0.85
Bunch peak current [A]	40.85	40.85

(a) Normalized emittance $\varepsilon_n = 3.75 \cdot 10^{-6}$[mrad], betatron amplitude $\beta_{h,v} = 128$[m].

2.3 PS (Case 3) and LEAR (Case 4) proton beam parameters

	Case 3	Case 4
Proton momentum GeV/c	26	0.31
ß value	0.993	0.3124
rms radius: Δ_r [mm]	1 (b)	2 (c)
rms bunch length: Δ_s [m]	0.674	No
Distance between bunches [m]	7.5	No
Number of particles per bunch: n_b	10^{11}	10^{10}
Number of bunches: n_0	84	1
Circumference [m]	628	78.59
Average current [mA]	642	2

(b) : $\varepsilon_n = 3 \cdot 10^{-6}$[mrad], $\beta_{h,v} = 10$[m], (c) : $\beta_{h,v} = 4$[m].

2.4 Ion beam parameters

A: Atomic mass, therefore the ion mass m = A·m_p
Z: Atomic charge, therefore the ion charge Q = Z·q
The type of ion is Mg with A = 24 and Z = 12
U_S: Voltage [V] between the ion source output and ground
v: Ion velocity [m·s^{-1}].

Most of the ion beam parameters will have no index while, if necessary, the proton beam parameters will be indexed by "p".

2.5 Electrical and magnetic field of the proton beam

We consider a proton beam that has a transverse Gaussian distribution and an uniform longitudinal distribution over the length: $L_b = \Delta_s\sqrt{2\pi}$. This is about the case of coasting beams and will be used hereafter even for "bunched beams" to serve as a simple illustration of the principle.

The proton bunch distribution "n[m^{-3}]" is given by:

$$n = \frac{n_b}{2 \cdot \pi} \frac{2}{{\Delta_r}^2 \cdot L_b} \exp\left(-\frac{r^2}{{\Delta_r}^2}\right). \qquad (2.1)$$

with $\int_0^r \xi \cdot \exp-\left(\frac{\xi}{\Delta_r}\right)^2 \cdot d\xi = \frac{{\Delta_r}^2}{2}\left[1 - \exp\left(-\frac{r^2}{{\Delta_r}^2}\right)\right]$

2.5.1 *Electrical field*

Using the Gauss theorem we obtain the radial electrical field:

$$E_r = \frac{2 \cdot n_b \cdot q}{4 \cdot \pi \cdot \varepsilon_o} \frac{1}{L_b} \frac{1}{r} \left[1 - \exp\left(- \frac{r^2}{\Delta_r{}^2} \right) \right] = V_o \, \Theta(r) \qquad (2.2)$$

with: $V_o[\mathrm{V}] = \frac{2 \cdot n_b \cdot q}{4 \cdot \pi \cdot \varepsilon_o} \frac{1}{L_b}$ *and* $\Theta(r)[\mathrm{m}^{-1}] = \frac{1}{r} \left[1 - \exp\left(- \frac{r^2}{\Delta_r{}^2} \right) \right]$.

2.5.2 *Magnetic field*

The proton beam current passing through a circle of diameter "r" is:

$$I = \frac{q \cdot n_b}{L_b} \left(1 - \exp\left(- \frac{r^2}{\Delta_r{}^2} \right) \right) \beta_p c; \qquad \beta_p = \frac{v_p}{c} .$$

The azimuthal magnetic field:

$$\vec{B}_\phi = \frac{\mu_o}{2\pi} \frac{q \cdot n_b}{L_b} \Theta(r) \beta_p \cdot c \cdot \vec{u}_\phi = B_\phi (- \sin\theta \cdot \vec{i} + \cos\theta \cdot \vec{j}) \qquad (2.3)$$

with $B_\phi = \frac{1}{4 \cdot \pi \cdot \varepsilon_o} \frac{2 \cdot q \cdot n_b}{L_b} \Theta(r) \frac{\beta_p}{c} = \frac{\beta_p}{c} E_r$

The magnetic field is maximum when E_r is maximum.

2.5.3 *Properties of the proton beam transversal electrical field and potential*

The transverse electrical field, given by Eq. (2.2) is maximum for a value $r = r_m$ such that:

$$\left(1 + 2 \frac{r_m{}^2}{\Delta_r{}^2} \right) \exp\left(- \frac{r_m{}^2}{\Delta_r{}^2} \right) = 1$$

and therefore for $r_m \cong \Delta_r$ (the exact value is $r_m = 1.121 \cdot \Delta_r$).

The transverse electrical field as a function of the radius is plotted in Fig. 2 for "Case 1". One sees that its maximum value is about $E_r(\mathrm{max.}) = 1.6 \cdot 10^6$ V/m. For $r >> \Delta_r$ the radial electrical field: $E_r \propto 1/r$. For $r \cong r_m$ the maximum p-beam magnetic field is about 50 Gauss which is significative.

The potential can be computed from the expression of the electrical field (2.2):

$$E_r = - \frac{dV}{dr} \Rightarrow V(r) = C - V_o \int_0^r \Theta(\psi) \, d\psi \qquad (2.4)$$

C[V] is a constant such that $V(\infty) = 0$. The potential V (obtained from the integration of the electrical field represented in Fig. 2) is plotted in Fig. 3 for C = 0. The maximum potential is about $5 \cdot 10^3$ V. Therefore the ion beam kinetic energy must be larger than $Q \cdot V(\text{max.}) \cong 5$ keV, if we want to have significant measurements of its deviation by the proton beam.

3. PROFILE MEASUREMENT WITH A POSITIVE ION PENCIL BEAM

The principle is shown in Fig. 4:

- An ion source provides a beam of small diameter (< 30 μm) at a relatively low velocity along the x-axis.
- At the source output the ion beam (i-beam) is displaced vertically (z-axis) and directed towards the proton beam (p-beam) which is centered at (0,0) and is moving at velocity v_p along the s-axis.
- Owing to the space-charge forces induced by the p-beam, the ions will be deflected by an angle θ and collected by the detector which, for simplicity, will be considered as consisting of horizontal strips at different ordinate z_f.

Since the deflection angle θ is a function of the initial i-beam ordinate $z_0 = z(t = 0)$, the relation between z_f and $z(t = 0)$ should allow us to retrieve the proton beam distribution.

3.1 Ion beam equations of motion

The ion having a velocity $\vec{v} = v_x \cdot \vec{i} + v_z \cdot \vec{j} + v_s \cdot \vec{k}$ will be subjected to the force $\vec{f} = Q(\vec{E} + \vec{v} \Lambda \vec{B})$, with $Q = Z \cdot q$ being the ion charge.

The equations of motion will therefore be:

$$\begin{aligned} \frac{dx^2}{dt^2} &= \frac{Q}{m} E_r \frac{x}{r}\left[1 - \frac{\beta_p \cdot v_s}{c}\right] \\ \frac{dz^2}{dt^2} &= \frac{Q}{m} E_r \frac{z}{r}\left[1 - \frac{\beta_p \cdot v_s}{c}\right] \\ \frac{ds^2}{dt^2} &= \frac{Q}{m} \frac{E_r}{r} \frac{\beta_p}{c}\left[v_x \cdot x + v_z \cdot z\right] \end{aligned} \qquad (3.1)$$

Remarks

Let the ion beam leave the source at location $(-x_S, 0, 0)$ with an initial velocity v_o, determined by the ion source potential U_S

$$v_o = \left(\frac{2 \cdot Q \cdot U_s}{m}\right)^{1/2}, \quad \vec{v}_o = v_o \cdot \vec{i} + 0 \cdot \vec{j} + 0 \cdot \vec{k}.$$

We suppose that the potential V due to the p-beam at the ion source level is zero volt. At any point of its trajectory the conservation of energy law implies that:

$$v_o^2 - \frac{2 \cdot Q \cdot V(r)}{m} = v^2;\ v^2 = v_x^2 + v_z^2 + v_s^2.$$

Therefore not only $v \leq v_0$ but also the ion initial kinetic energy must be larger than $Q \cdot V(r)$ for any value of r taken by the ion all along its trajectory. For small ion source voltage U_S, the ion velocity $v = \beta \cdot c$ is relatively small and therefore the terms in $(\beta_p/c) \cdot v_{pl}$, where the index "pl" stands for any plane, can be neglected. It is worth noticing that if, instead of an ion beam, we expect to use an electron beam the corresponding initial velocity v_{eo} at the source output will be larger since

$$\frac{v_o^2}{v_{eo}^2} = \frac{m_e}{m_p}\frac{Z}{A}, \text{ where } m_e = 9.1 \cdot 10^{-31} \text{ kg is the electron mass.} \qquad (3.2)$$

Therefore the electron beam would be significantly influenced by the p-beam azimuthal magnetic field.

Using thus a low energy ion pencil beam one comes to a simplified set of equations:

$$\frac{dv_x}{dt} = \frac{dx^2}{dt^2} = \frac{Q}{m} E_r \frac{x}{r}$$

$$\frac{dv_z}{dt} = \frac{dz^2}{dt^2} = \frac{Q}{m} E_r \frac{z}{r} \qquad (3.3)$$

$$with : E_r = V_o \Theta(r).$$

3.2 Rough estimate of the deflection angle θ (Fig. 4)

Let us consider a small deviation "θ" so that the ion beam remains on the $z = z_0$ line starting from $x_S = -x_f$ (source abscissa) to end up at x_f (detector abscissa).

The transverse electrical field component $E_\perp$ along the z_0 axis is given by :

$$E_\perp = E_r \frac{z_o}{r}.$$

The transverse force is thus

$$f_\perp = Q \cdot E_\perp = \frac{dp_\perp}{dt} = Q \cdot V_o \cdot z_o \frac{1 - \exp(-\frac{r^2}{\Delta_r^2})}{r^2}$$

with $p_\perp$ the transverse momentum, $r^2 = x^2 + z_o^2$ and $x = v_o \cdot t$. Integrating from $-x_f$ to x_f gives:

$$\Delta p_\perp = Q \cdot V_o \cdot z_o \int \frac{1 - \exp(-\frac{x^2 + z_o^2}{\Delta_r^2})}{x^2 + z_o^2} dt = \frac{Q \cdot V_o}{v_o \cdot z_o} \int_{-x_f}^{x_f} \frac{1 - \exp(-\frac{z_o^2}{\Delta_r^2}(1 + \frac{x^2}{z_o^2}))}{1 + \frac{x^2}{z_o^2}} dx.$$

We set $\frac{z_o}{\Delta_r} = \zeta$, $\frac{x}{z_o} = u$, $u_f = \frac{x_f}{\Delta_r} >> 1$, $z_o \neq 0$ to finally obtain:

$$\Delta p_\perp = \frac{Q \cdot V_o}{v_o} \int_{-u_f}^{u_f} \frac{1 - \exp(-\zeta^2(1+u^2))}{1+u^2}\, du = \frac{Q \cdot V_o}{v_o} I(\zeta). \qquad (3.4)$$

The integral $I(\zeta)$ is represented by Fig. 5. From this curve [but also from Eq.(3.4)] it appears clearly that for: $\zeta \geq 2 \quad I(\zeta) \Rightarrow \pi$.

Therefore the asymptotic deflection angle θ_{max} is:

$$\theta_{max} = \frac{\Delta p_\perp}{m \cdot v_o} = \frac{\pi \cdot Q \cdot V_o}{m \cdot v_o^2} = \frac{\pi}{2} \frac{V_o}{U_s}. \qquad (3.5)$$

Numerical application: "Case 1", $V_o = \frac{2 \cdot n_b \cdot q}{4 \cdot \pi \cdot \varepsilon_o} \frac{1}{L_b} = 2.447 \cdot 10^3$ Volt,

$U_s = 10^4[V] \Rightarrow \theta_{max} = 0.32$ rad,

for: $U_s = 2.5 \cdot 10^4[V] \Rightarrow \theta_{max} = 0.154$ rad,

$U_s = 5 \cdot 10^4[V] \Rightarrow \theta_{max} = 7.6 \cdot 10^{-2}$ rad.

3.3 Simulations with unbunched beams

We consider mainly the numbers of the Case 1 parameters but we neglect the effects of a limited bunch length L_b. More precisely the p-beam has a Gaussian transverse distribution, with rms radius Δ_r. It has a longitudinally uniform distribution over $L_b = \Delta_r \cdot \sqrt{2\pi}$, and does not move when crossing the ion beam. Therefore we use for E_r the expression given in Section 2.5.1, Eq. 2.2. This is not a realistic case, except for coasting beams, but is considered here in order to illustrate the principle.

Figure 6 shows an example of ion trajectories z(x) as a function of the initial ordinate z_0 and for an ion source voltage $U_S = 5.10^4$ V. The p-beam, of rms radius Δ_r = 1mm is at position (0,0). In Fig. 7 are plotted the deflection angles $\theta(z_o)$[rad], with $\theta = \arctan(v_{zf}/v_{xf})$, where the index f denotes the final values of the velocities *i.e* those at the time of arrival of the ion on the detector strip, for different values of U_s. From these curves one sees first a quite linear increase of θ with z_0 followed by a saturation for values of $z_0 \geq \Delta_r$. The value z_0 giving the maximum angle of deviation is a rough estimate of the transverse rms radius Δ_r. The maximum angle of deviation is comparable with the estimations made in Section 3.2, Eq. 3.5.

In Fig. 8 the voltage U_S is reduced to $5 \cdot 10^3$ V illustrating that, owing to the relative large p-beam space charge potential, the i-beam cannot reach the detector; this is in agreement with what has been mentioned in the remark of Section 3.1.

The study of Case 3 is immediate. In that case E_r(max.) = $1.1 \cdot 10^5$ V/m and the space-charge voltage is about 500 V.

The Case 4, where our assumptions are satisfied since the beam is coasting, has also been computed. This is of limited interest since the p-beam space-charge potential is about 1 V and therefore of the same order as the variation in source energy.

3.3.1 Influence of the ratio Z/A

From Eq. 3.3 and considering small angle deviations

$$\Delta V_z = \int_{t_{initial}}^{t_{final}} \frac{Q}{m} E_r \frac{z}{r} dt \cong \frac{Q}{m \cdot v_o} \int_{x_{initial}}^{x_{final}} E_r \frac{z}{r} dx.$$

The deviation angle

$$\theta = \frac{\Delta v_z}{v_o} \cong \frac{Q}{m \cdot v_o^2} \int_{x_{initial}}^{x_{final}} E_r \frac{z}{r} dx = \frac{1}{2U_s} \int_{x_{initial}}^{x_{final}} E_r \frac{z}{r} dx$$

is, to the first order, independent of the ratio Z/A.

3.4 Bunched proton beam

As seen in Cases 1 and 2, the LHC has to cope with bunches having a length L_b much smaller than the distance between them. Therefore, the time of interaction between the i-beam and the p-bunch is significantly reduced (with respect to that relative to the assumptions made in Section 3.3). The simulations made in Section 3.3 have to be refined including the longitudinal Gaussian distribution of the bunch (with rms length Δ_S).

Equation (2.1) has to be modified such that the proton-bunch density n is now

$$n[\mathrm{m}^{-3}] = \frac{n_b}{(2 \cdot \pi)^{3/2}} \frac{2}{\Delta_r^2 \Delta_s} \exp\left(-\frac{r^2}{\Delta_r^2}\right) \exp\left(-\frac{s^2}{2\Delta_s^2}\right) \tag{3.6}$$

with Δ_s[m] being the rms length of the longitudinal distribution.

In the case of relativistic beams, the E-field, at any value of s, is mainly radial. Equation (2.2) must be modified in order to introduce the longitudinal Gaussian distribution, giving:

$$\begin{aligned} E_r &= \frac{2 \cdot n_b \cdot q}{(2\pi)^{1/2} 4 \cdot \pi \cdot \varepsilon_o} \frac{1}{\Delta_s} \Theta(r) \exp\left(-\frac{s^2}{2\Delta_s^2}\right), \\ E_r &= V_o \cdot \Theta(r) \cdot \exp\left(-\frac{s^2}{2\Delta_s^2}\right); \qquad s = c \cdot t. \end{aligned} \tag{3.7}$$

This modified equation for E_r can now be used to solve Eq. (3.3).

3.4.1 Simulations

We know that the proton time-dependent longitudinal position is defined by $s = \beta_p \cdot c \cdot t \cong c \cdot t$. In order to have an effective interaction between the ion and the p-beam bunch these particles must meet, in the neighborhood of (0,0), at about the same time "t". Therefore one has to offset the time t in the proton equation by "t_O" such that

$\frac{|x_s|}{v_o} \cong t_o$, with x_S the abscissa of the ion source or that of the ion at t = 0[s]

and $v_o = \sqrt{\frac{2QU_s}{m}}$ the ion initial velocity along the x-axis (Fig. 9).

Thus at a given time "t" the transverse electrical field seen by the ion at radius $r = \sqrt{x^2 + z^2}$ is

$$E_r(r,t) = V_o \cdot \Theta \cdot (r) \exp\left(- \frac{\left(c(t - t_o)\right)^2}{2\Delta_s^2} \right). \qquad (3.8)$$

The set of curves given in Fig. 10 shows the area covered by the ion trajectories for: $U_S = 10^4$ V, $z_O = 2$ mm, different initial values of t_O and for Case 1. Corresponding to Fig. 10 Table 3.1 gives ϕ or different values of t_O. As expected ϕ passes through a maximum for a given value of t_O.

Using the data from Figs. 2 and 3 one sees that the ion beam would feel the p-beam forces over an interval of about $[-5\cdot\Delta_r, 5\cdot\Delta_r]$ and therefore during the time interval: $\Delta t_i = (10\Delta_r)/v_o \cong 10^{-8}$ s for $v_o = 10^6 \text{ m} \cdot \text{s}^{-1}$. The p-beam will "see" the ion beam during the time interval : $\Delta t_p = L_b/v_p = 6.3 \cdot 10^{-10}$ s for $v_p = c$. Since $\Delta t_p << \Delta t_i$ the change in transverse momentum $\Delta p_\perp = \int f_\perp \cdot dt_p$ will thus be less than one computed in Section 3.3. It is reduced by a factor about equal to $v_o \cdot \Delta t_p \,/\, \Delta_r$. Under the conditions of Case 3 the reduction will be less since the bunch length is relatively large. In any case the deviation angle can be increased by reducing U_S (even to voltages U_S of the order 5.10^3 V, if we consider Case 1).

For bunched beams it is preferable to look for the maximum deviation angle. The maximum angle θ_m is given in Table 3.2 as a function of z_O, for $U_S = 5.10^4$ V and for Case 1. $\theta_m(z_o)$ has the same shape as that represented by Fig. 7. Again, as for the unbunched case, θ is maximum for $z_o \cong \Delta_r$.

3.4.2 Signal treatment

As a consequence of the short p-bunch length, the current distribution on the detector (when the ion source delivers a continuous current at constant ordinate z_O) has the shape shown in Fig. 11.

In order to reduce the disturbances, introduced by the background signals, several techniques may be used:

a) Measurements of the maximum deflection, or more precisely of $(z\text{-}z_O)$(max.).
b) Use of gated electronics synchronized with the passage of the p-beam bunch.

c) Scanning of the ion beam, across a small hole, by a fast electrostatic deflector at the p-bunch repetition rate (Fig 12). This will provide a bunch of ions synchronized with the p-bunch to be measured.

3.5 Detector and ion source

3.5.1 Detector

On their way from the source to the detector the ions will be influenced by their own space-charge forces. This will increase the i-beam diameter.

For a uniform ion distribution the increase in radius Δ_{ri} :

$$\Delta_{ri} = \frac{Q}{m \cdot \gamma^3} \frac{1}{4 \cdot \pi \cdot \varepsilon_o} \frac{I}{v_o^3} \frac{\Delta x^2}{a} \tag{3.9}$$

where I is the ion beam intensity
Δx is the distance between the ion source and the detector
a is the initial beam radius .

Example:

$U_s = 5 \cdot 10^4 V \Rightarrow v_o = 2.18 \cdot 10^6 \mathrm{m} \cdot \mathrm{s}^{-1}$, $\gamma \equiv 1$,
$a = 5\,\mu\mathrm{m}$, $\Delta x = 5\mathrm{cm}$, $\Delta_{ri} = a$,
gives $I = 0.24\mu\mathrm{A}$ ($I = 0.024\mu\mathrm{A}$ *for* $U_s = 500\mathrm{V}$, Case 3).

In the case of an electron beam one comes to the intensity of 1.2 μA.

Such a rather low intensity may imply that the detector has to be used in counting mode. One can also make use of MCP amplification (if the Micro-Chanel Plate has a good efficiency) in order to obtain a total resolution (including the ion beam vertical resolution Δz_o) of about $0.1 \cdot \Delta_r$.

3.5.2 The ion source

The Liquid-Metal Ion Source (LMIS) can be chosen for our purpose (Fig. 13). It generates a beam with all the required parameters and precisions.

Its principle is based on the ion emission from a liquid conducting surface, as a result of a very high electrical field (E ~ 2.10^8 V/cm). In spite of a relative low operational voltage (U ~ 10^3 to 10^4 V) such a high field exists near the "*liquid edges*" the curvature of which can be less than 15 Å.

The LMIS emitter is a needle with point radius of about 3 - 15 μm. Ions are emitted from that point. The thick part of the needle is immersed in a cylinder containing the molten metal which is fed towards the point along the lateral surface. The overall system is heated from outside to the required temperature. The operation voltage and emission current ranges are 5 - 15 kV and 0.5 - 200 μA respectively. A higher ion energy can be obtained by an additional acceleration. The beam diameter and current are controlled by an extractor (a diaphragm with a hole) located at the opposite end of the needle.

A wide range of metals (from Li to Bi) can be used as feed material. The choice of the type of ion will depend on many parameters. For the present report we chose Mg.

The optical system used for beam steering and focusing consists of accelerating electrodes, an electrostatic lens, and scanning plates.

This type of source should allow us to foresee an ion beam with a diameter ranging between 1 and 10 μm at the level of the p-beam to be sensed.

4. PROFILE MEASUREMENTS WITH A NEUTRAL BEAM

The positive ion beam, of rectangular or round cross-section, can be neutralized by a "Neutralization cell" placed immediately at the ion source output (Fig. 14). The main difficulty may come from the effect on the proton beam vacuum system. The result of the interaction of the neutral beam with the proton beam can be used in two ways (for our purpose):

- Detection of the secondary particles (γ particles) by a scintillator placed outside the proton beam pipe. This is equivalent to the principle of the classical fast beam scanner using carbon or beryllium fibers [Ref. 3].

- Detection of the fraction of the neutral particles being ionized by the proton beam.

4.1 Detection of secondary gamma particles

The classical Beam Profile Wire Scanner (BWS) making use of a thin carbon fiber induces too much disturbance on the LHC environment for high-energy beams [4].

A possible way to reduce these disturbances could consist in the use of a neutral beam instead of the carbon fiber. The neutral beam will have a much lower density than the carbon wire, leading to less interactions. Also the neutral beam trajectory will not be disturbed by the large proton beam space-charge forces.

The same principle could be used with a source able to provide small diameter neutral bullets (private communication from J.B. Jeanneret).

4.1.1 Principle

We consider a neutral beam crossing transversally (in the horizontal or vertical plane) the proton bunch at different positions "z_0" from the bunch longitudinal axis (Fig. 15 a,b). The transverse position z_0 is expected to be adjusted as mentioned in Section 3.

The interactions between the neutral beam and the relativistic proton beam will produce high-energy gamma particles.

The gamma particles emitted, at small angle, from the neutral beam target will traverse a scintillator placed at a distance L from the γ source (Fig. 15a). The voltage, measured across a resistance R_{pm} at the output of a photo-multiplier (PM) connected to the scintillator, will be proportional to the number of protons that have interacted with the neutral beam. By changing "z_0" one can therefore retrieve the proton beam transverse distribution.

We aim to make a rough estimate of the required neutral beam source and of the detector (scintillator + photo-multiplier) in order to cope with the required accuracies.

All the numerical applications (N.A) will be made for an LHC proton beam corresponding to Case 1 and using the following data and parameters.

4.1.2 Data, parameters

-Neutral target beam:

Cesium : Cs, A = 133, Z = 55, $m_{cs} = A \cdot m_p = 2.22 \cdot 10^{-25}$ kg,
Cs beam dimensions at the source output: h = 1 cm, d = 10 μm = 10^{-3} cm, or diameter ϕ = 30 μm,
Current density $J_{cs} = 5\,\mathrm{mA/cm^2}$,
Kinetic energy $E_{cs} = 10\,\mathrm{keV}$,
Nuclear cross-section $\sigma = 1.3$ barn. Ionization cross-section $\sigma_i = 10^{-18}\,\mathrm{cm^2}$.

-Scintillator and PM parameters:

Scintillator:

Type: CsI
Linear attenuation: $\mu[\mathrm{cm}^{-1}] = 0.2$
Dimensions : Inner diameter: 56 mm,
Outer diameter: 256 mm,
Thickness: 5 cm
Distance from the γ particle source to the scintillator: L = 20 m.

PM

Gain: $G_{pm} = 10^6$,
Output resistance: $R_{pm} = 1$ MΩ,
Efficiency: Emission of 1 photo-electron for 1 keV lost by the particle in the scintillator.

4.1.3 Neutral beam source

We consider a single charged Cesium " Cs" beam having a rectangular cross-section with h = 1 cm and d = 10 μm (Fig. 15.b). The ions move transversally (with respect to the proton beam) with a velocity v_{cs} and therefore a kinetic energy E_{cs} such that :

$$v_{cs} = \sqrt{\frac{2E_{cs}}{m_{cs}}}.$$

An example of an ion source can be taken from Ref. [2]. We consider a beam of Cesium atoms, at kinetic energy $E_{cs} = 10\,\mathrm{keV}$, extracted from a hot plate with current density $J_{cs} = 5\ \mathrm{mA/cm^2}$ (Fig. 14). The Cs beam passes a first slit having the dimensions h and d defined before. The ion temperature at the level of this first plate is about 0.1 eV such that the angular spread in the beam is about $\sqrt{0.1/10.000} = 3$ mrad. If one places an identical second slit, with the same dimensions (h,d) at a distance $l = 10$ cm from the first, the angular spread at the output will be about:

$$\psi = \frac{d}{2}\frac{1}{l} = 0.15 \text{ mrad}.$$

This will result in a beam with d' = 30 μm at a distance of 20 cm from the second slit where the Cs beam is expected to cross the proton beam.

After the second slit the Cs beam passes through a neutralization cell using resonant charge exchange. We assume 100% beam neutralization. The angular spread caused by the resonant charge exchange is the momentum of the outer electron divided by the ion momentum. Since the electron-to-ion mass ratio is around 240.000 and the energy ratio 5 eV/10.000 eV one obtains an average scattering angle

$$\sqrt{\frac{5}{10.000}}\,\frac{1}{240.000} \cong 0.5\ \mu\text{rad}$$

which can be neglected.

The density of neutral ions n_{cs} at velocity v_{cs} is:

$$n_{cs}[\text{m}^{-3}] = \frac{1}{e}\,\frac{I_{cs}}{h \cdot d}\,\frac{1}{v_{cs}} = \frac{J_{cs}}{e}\,\frac{1}{v_{cs}}$$

For 10 keV ions:

$$v_{cs}[\text{ms}^{-1}] = \sqrt{\frac{2e \cdot 10^4}{m_{cs}}} = 1.2 \cdot 10^5$$

$$n_{cs}[\text{m}^{-3}] = \frac{5 \cdot 10^{-3} \cdot 10^4}{1.6 \cdot 10^{-19}}\,\frac{1}{1.2 \cdot 10^5} = 2.6 \cdot 10^{15}.$$

This can be compared to the density of a carbon fiber:

$$n_c = \frac{\rho[\text{kg/m}^3] \cdot \text{Avogadro number}}{A_c} = \frac{2.3 \cdot 10^3 \cdot 6.02 \cdot 10^{23}}{12} = 1.15 \cdot 10^{26}$$

showing that the LHC environment will be less disturbed when using the low density Cs beam [4].

An alternative way to produce scanned atomic beams consists in the use of a negatively charged ion beam which is stripped after passing the scanning system. LMIS of negative ions, which fulfils our requirements are available (V. Dudnikov, INP Novosibirsk, private communication).

4.1.4 Number of secondary gamma particles

The probability that a proton will undergo a nuclear interaction with the Cs neutral beam is given by:

$$p_r = \sigma\, n_{cs}\, h = 3.38 \cdot 10^{-15}$$

Let the proton beam have a transverse Gaussian distribution of rms value $\Delta_r[\text{m}]$ such that its transverse distribution can be expressed by:

$$\frac{dN}{dz} = \frac{n_b\, n_o}{\sqrt{2\pi}\Delta_r} \exp\left(-\frac{z^2}{\Delta_r{}^2}\right), \qquad \text{with } \Delta_r = \sqrt{\frac{\varepsilon_n\, \beta_{h,v}}{\beta\gamma}} \text{ the rms width and } \beta_{hv} \text{ the}$$

betatron amplitude.

The number of protons passing every second through the neutral target, of height $d' << \Delta_r$ is therefore:

$$\dot{n}_p = \frac{n_b\, n_o}{\sqrt{2\pi}} \frac{d'}{\Delta_r} f_r \exp\left(-\frac{z^2}{2\Delta_r{}^2}\right), \qquad \text{with} \qquad d' = 30\ \mu m.$$

N.A: $\sigma_y = 1$ mm, $z = 0$ gives $\dot{n}_p = 6 \cdot 10^{16}$ protons/s.

Thus the number of nuclear events per second is:

$$\dot{n}_{ev} = p \cdot \dot{n}_p$$

N.A : $\dot{n}_{ev} = 2 \cdot 10^2$.

At 0.45 TeV the number of secondary gamma particle per nuclear event is 4.553 and their energy $E_\gamma = 16.472$ [GeV] [4]. Therefore the total number of gamma particles emitted per second is:

$$\dot{n}_\gamma = 4.453 \cdot \dot{n}_{ev}$$

N.A : $\dot{n}_\gamma = 920 \cong 1000.$

The gamma particles are emitted in an angle (which depends upon the proton energy) of rms value $\theta_\gamma << 1$. The angular distribution is expected to be Gaussian:

$$\frac{d\dot{n}_\gamma}{d\theta} = n_\gamma \frac{1}{\sqrt{\pi}\,\theta_\gamma} \exp\left(-\frac{\theta^2}{\theta_\gamma{}^2}\right).$$

Let the scintillator, at distance L = 20m from the emission point , have an inner diameter of 56 mm and an outer diameter of 256 mm. This will correspond to the angles:

$$\theta_{min} = 28 \cdot 10^{-3}/20 = 1.4\,\text{mrad},\ \theta_{max} = 128 \cdot 10^{-3}/20 = 6.4\,\text{mrad}.$$

The number of gamma particles passing through the scintillator every second is therefore given by:

$$d\dot{n}_{\gamma sc} = \dot{n}\gamma \left[\frac{1}{\sqrt{\pi}\,\theta_\gamma} \int_{\theta_{min}}^{\theta_{max}} \exp - \left(\frac{\theta^2}{\theta_\gamma{}^2}\right) d\theta\right].$$

N.A: $\theta_\gamma = 10$ mrad, $\theta_{max} / \theta_\gamma = 0.64$, $\theta_{min} / \theta_\gamma = 0.14$.

The term within square bracket is equal to 0.478 such that $\dot{dn}_{\gamma sc} = 440$.

The gamma particle, at energy E_γ, traversing the scintillator of thickness d_{sc} will lose an energy ΔE_γ:

$$\frac{\Delta E_\gamma}{E_\gamma} = 1 - \exp(-\mu \cdot d_{sc}) = 0.632$$

and therefore the energy lost per second by all the gamma particles passing through the scintillator is:

$$\Delta W = \dot{dn}_{\gamma sc} \cdot \Delta E_\gamma$$

N.A: $\Delta W = 440 \cdot 0.632 \cdot 16.472 = 4.600[\text{GeV}]$.

Photo-multiplier :

As a rough approximation (from the measurements with anthracene scintillators) one can estimate that about one photo-electron will be generated for a loss of 1 keV in the scintillator. Introducing now the photo multiplier gain G_{pm} the voltage on the PM output resistor is:

$$V_{pm} = R_{pm} \cdot I_{pm} = R_{pm} \cdot G_{pm} \cdot \Delta W[\text{keV}] \cdot q$$

N.A: $V_{pm} = 0.74[\text{V}]$ which is comfortable, though our numbers refer to the peak amplitude and that one has to consider the voltages to be detected when the neutral beam crosses the edges of the proton bunch. The measurement over a period of 1 s will of course reduce the effects of electronic noise.

4.2 Detection of ionized particles

4.2.1 Principle

Now the neutral beam of diameter ϕ (therefore : $h = d = \phi$), when crossing the p-beam, is ionized. The ionized particles are deflected towards a detector connected to an electronic system operating in counting mode (Fig 16).

4.2.2 Number of ionized particles

The probability of ionization is:

$$pr_i = \sigma_i \, n_{cs} \, \phi.$$

The ionization cross-section σ_i is estimated from numbers given by the LHC vacuum experts. It is of the order of 10^{-18}cm^2. If we take : $\phi = d = 30\mu\text{m} = 3 \cdot 10^{-3}\,\text{cm}$ then:

$$pr_i = 10^{-18} \cdot 2.6 \cdot 10^{15} \cdot 3 \cdot 10^{-3} = 7.8 \cdot 10^{-6}.$$

The number of ionized particles per second when the proton beam is crossed at z = 0 is thus:

$$\dot{n}_i = \dot{n}_{ev} = pr_i \cdot \dot{n}_p = 4.7 \cdot 10^{11},$$

which will give an accurate measurement of the proton beam transverse profile. The ionized molecules will of course be deviated by the p-beam, as described in Section 3, but this is of little importance since one operates in counting mode and therefore register the integration of the ionized molecules.

5. CONCLUSION

The use of small-dimension charged or neutral beams interacting with the proton beam to be measured looks promising. A resolution of the order of 30 μm seems attainable.

The first method, using positive ion beams, presents few difficulties except for unforeseen perturbations.

The second method, using the ionization of neutral pencil beams, would give useful results. The main difficulties may come from the neutralization process itself which could introduce perturbations on the LHC vacuum system. This must be investigated.

References

[1] J.A. Pasour and M.T.Ngo, *Non perturbing Electron Beam Probe to diagnose charged-particle beams*, R.S.I 63 (1992) 3027.

[2] W.E. Nexsen et al , *Minimal Interference Beam Size/Profile measurement techniques applicable to the collider* (an exhaustive list of references can be found in this report),SSC-631 Report(May 1993).

[3] J. Bosser et al., *Transverse emittance measurement with a rapid Wire Scanner at the CERN SPS*, NIM A235(1985) 475-480.

[4] J. Bosser, *Some properties of the beam wire-scanner (BWS) foreseen for LHC*, PS/BD/Note 93-04 .

Distribution (of the Abstract):

PS Scientific ant Technical Staff.

Figure Captions

Figure 1 : System of coordinates. The target beam (positive or neutral pencil beams) is moving along the 0x (horizontal plane) or along the 0z(vertical plane). The proton beam is moving along the Os axis .

Figure 2 : Electrical field E_T[V/m] distribution versus the radius r[m]. "Case 1" ; the unbunched p-beam is at the center.

Figure 3 : Potential V[V] as a function of r[m] obtained by the integration of the electrical field represented by Figure 2.

Figure 4: Principle of the detector based on the deflection of a pencil beam by the proton beam . 1: Ion source, 2:Electrostatic steering electrodes, 3: Round proton beam of rms radius r moving perpendicular to the 0xz plane, 4: Horizontal strip line detector , 5: Proton beam vacuum chamber.

Figure 5: $$I(\zeta) = \int_{-u_f}^{u_f} \frac{1 - \exp(-\zeta^2 (1 + u^2))}{1 + u^2} du,\ \zeta = \frac{z_0}{\Delta_r},\ u_f = \frac{x_f}{z_o}.$$

Figure 6: Trajectory of the ion beam z = z(x) for different initial values z_0 of z. The proton beam of rms radius 1 mm is at the center (z = 0 , x = 0). Ion source potential $U_s = 5 \cdot 10^4$ V.

Figure 7: Ion beam deflection angle $\theta(z_o)$. for an unbunched proton beam *curve a*: $U_s = 5 \cdot 10^4$ V, *curve b*: $U_s = 2.5 \cdot 10^4$ V, *curve c*: $U_s = 10^4$ V.

Figure 8: Trajectory of the ion beam z = z(x) for different initial values z_o and $U_s = 5 \cdot 10^3$ V.

Figure 9: Representation of the geometrical position of the ion beam when leaving the source and of the proton bunch such as they meet at (0.0).

Figure 10: Trajectory z = z(x) for an initial position z_0 = 2 mm and different time offsets t_0.

Figure 11 : Signal observed on the strip-line detector at position z_f as a function of time.

Figure 12: Principle of the ion beam pulsing.

Figure 13 : Principle of the (LMIS) ion source. 1: needle, 2: meniscus of liquid, 3: container wall, 4: heater.

Figure 14 : Principle of the neutral Cs source.

Figure 15 : Principle of the particle detector.

Figure 16 : Principle of the Cs^+ detector.

Table 3.1 : t_0 and the deflection angle θ for z_0=2 mm and for a bunched p-beam (U_S=1 0^4V).

Table 3.2 : Maximum deflection angle as a function of z_0 for a bunched p-beam ($U_S = 10^4$V).

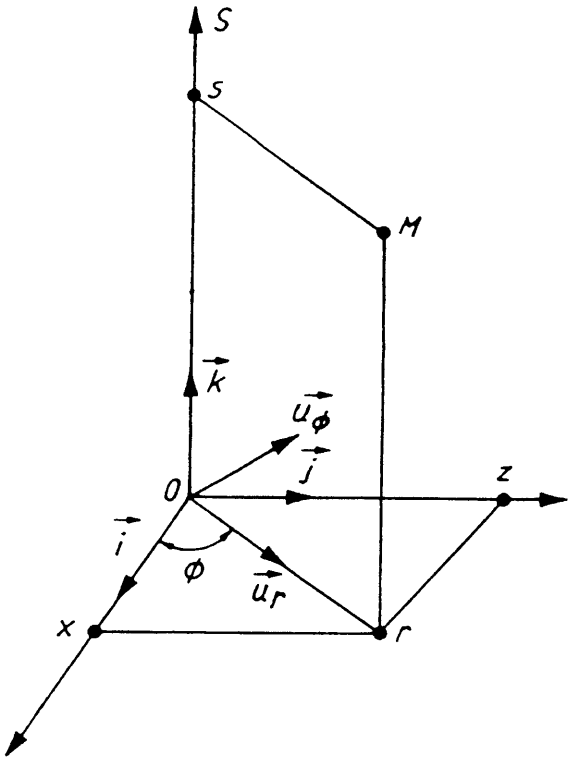

Figure 1

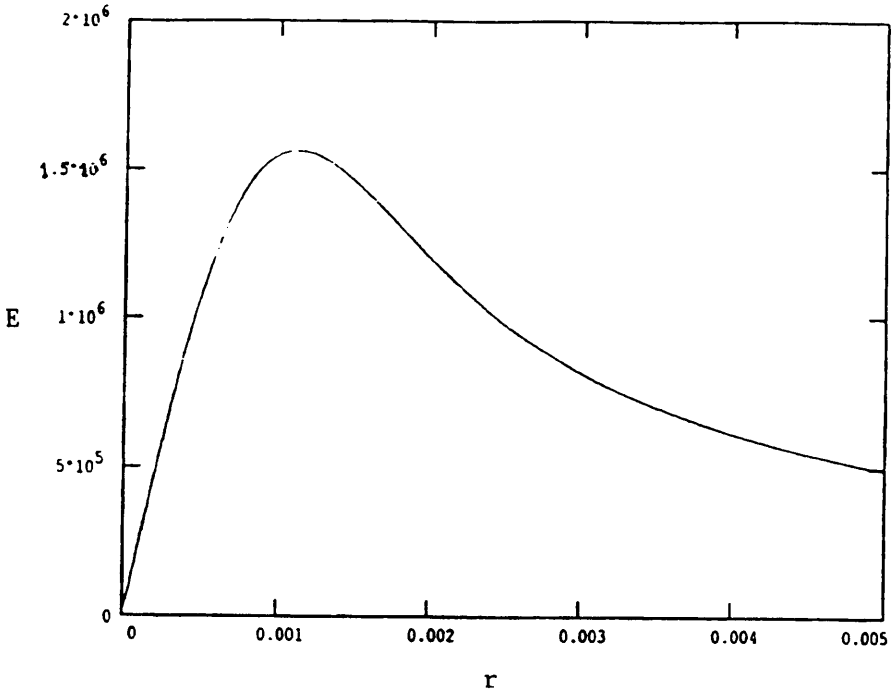

Figure 2

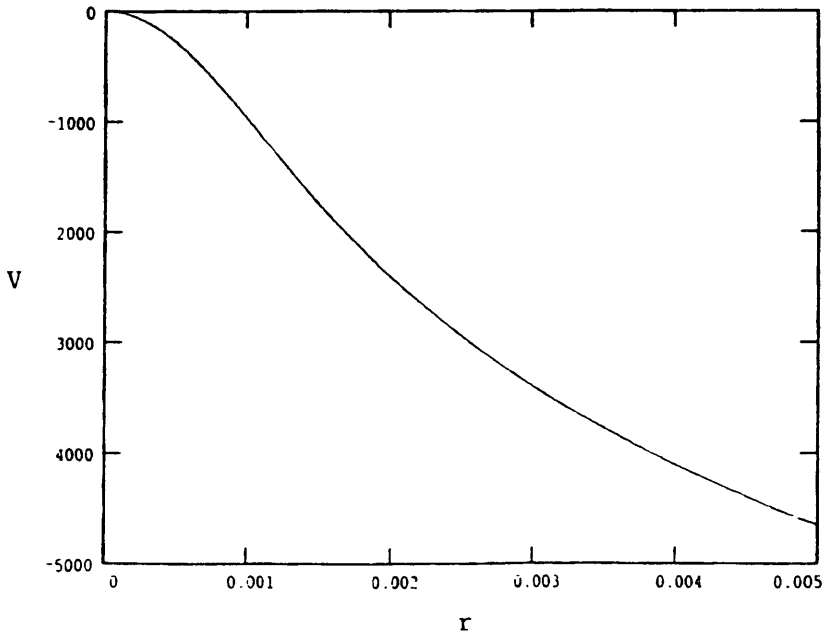

Figure 3

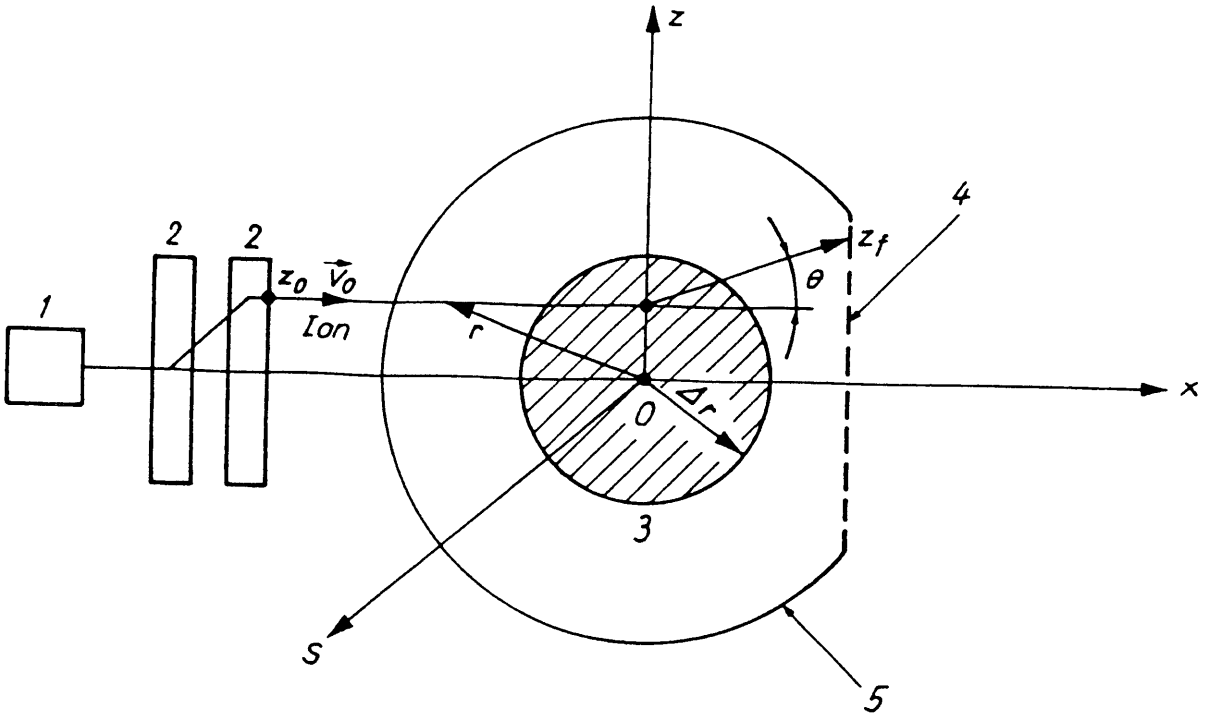

Figure 4

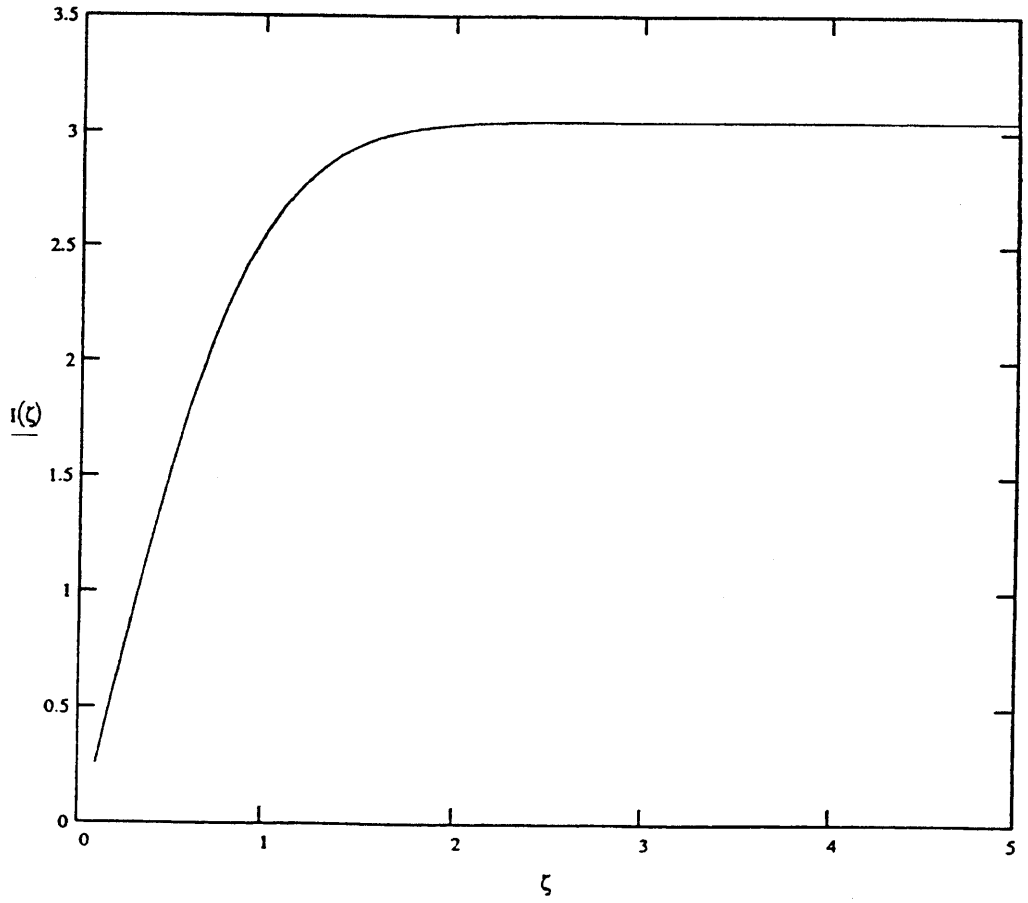

Figure 5

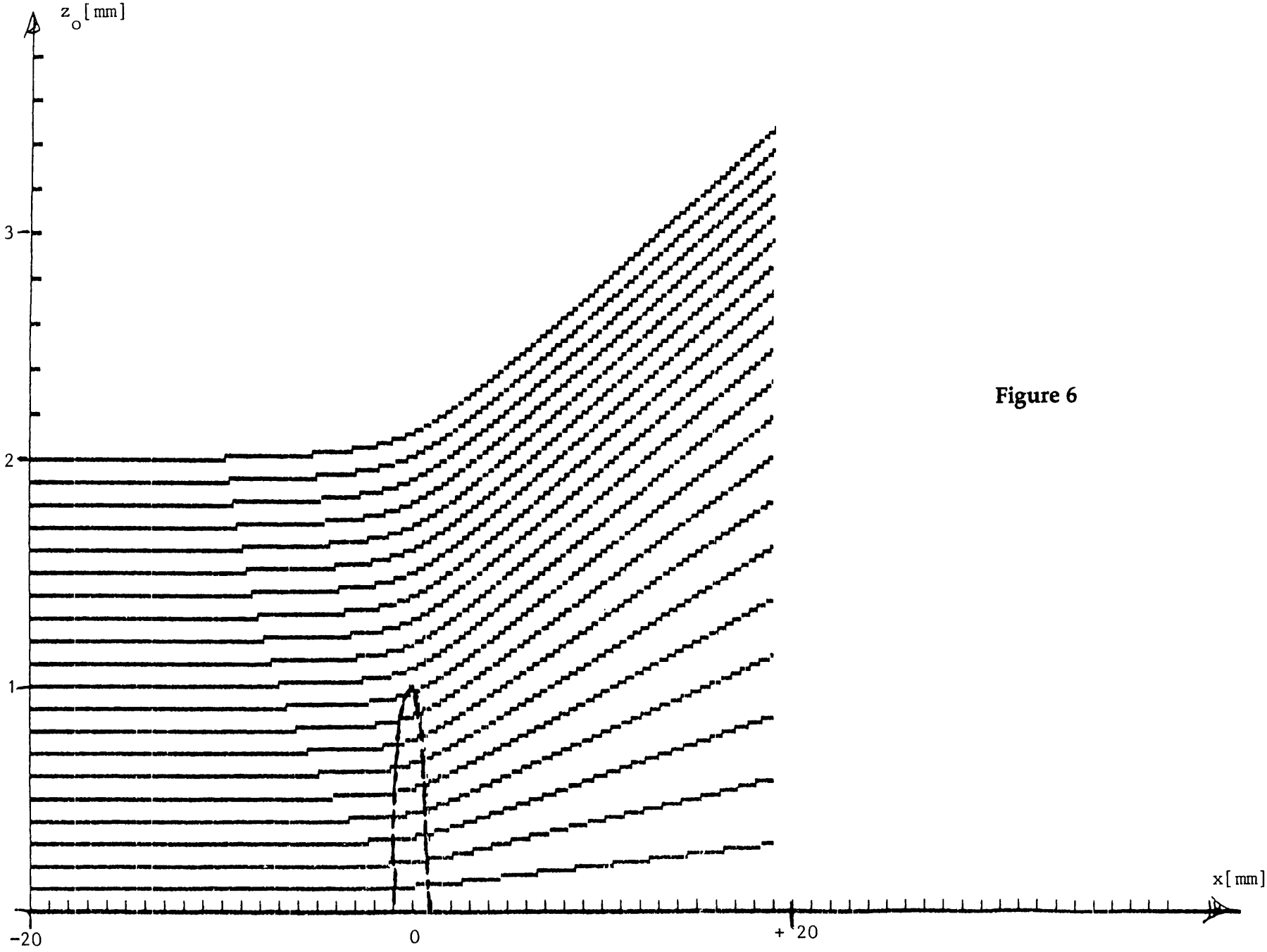

Figure 6

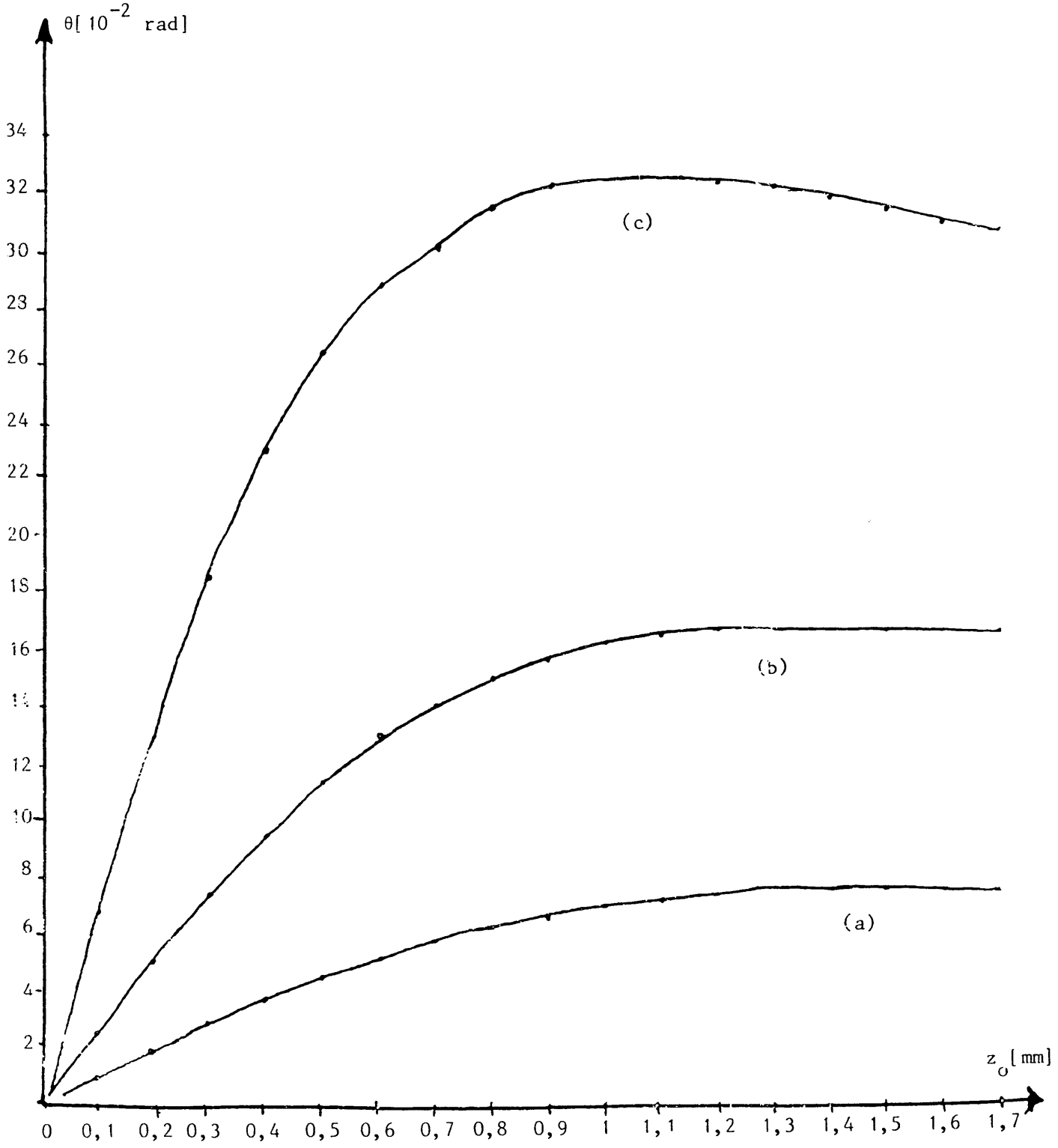
θ[10^-2 rad]
34
32
30
28
26
24
22
20
18
16
14
12
10
8
6
4
2
(c)
(b)
(a)
z_o [mm]
0
0,1
0,2
0,3
0,4
0,5
0,6
0,7
0,8
0,9
1
1,1
1,2
1,3
1,4
1,5
1,6
1,7

Figure 7

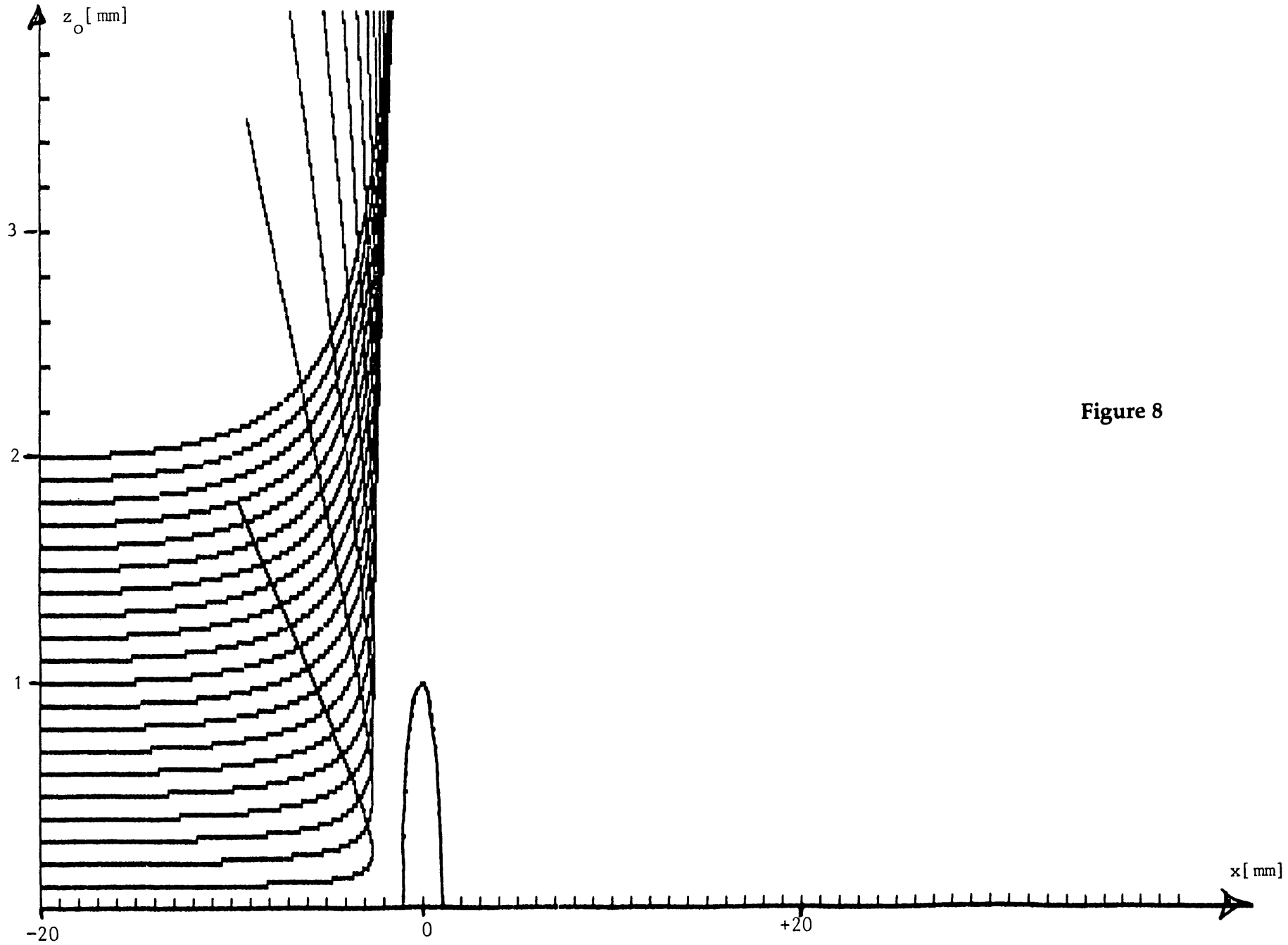

Figure 8

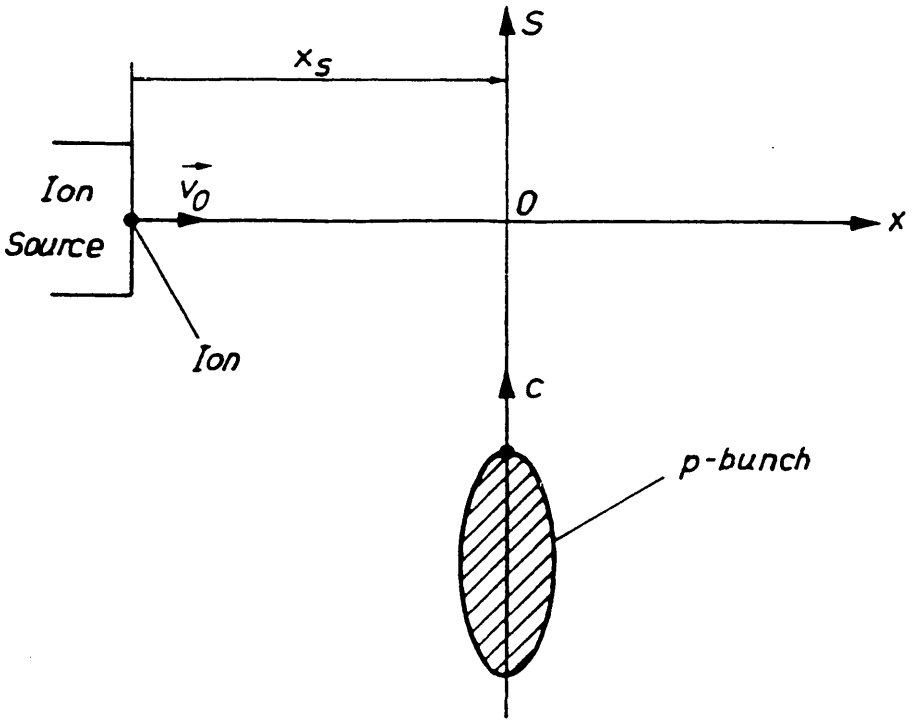

Figure 9

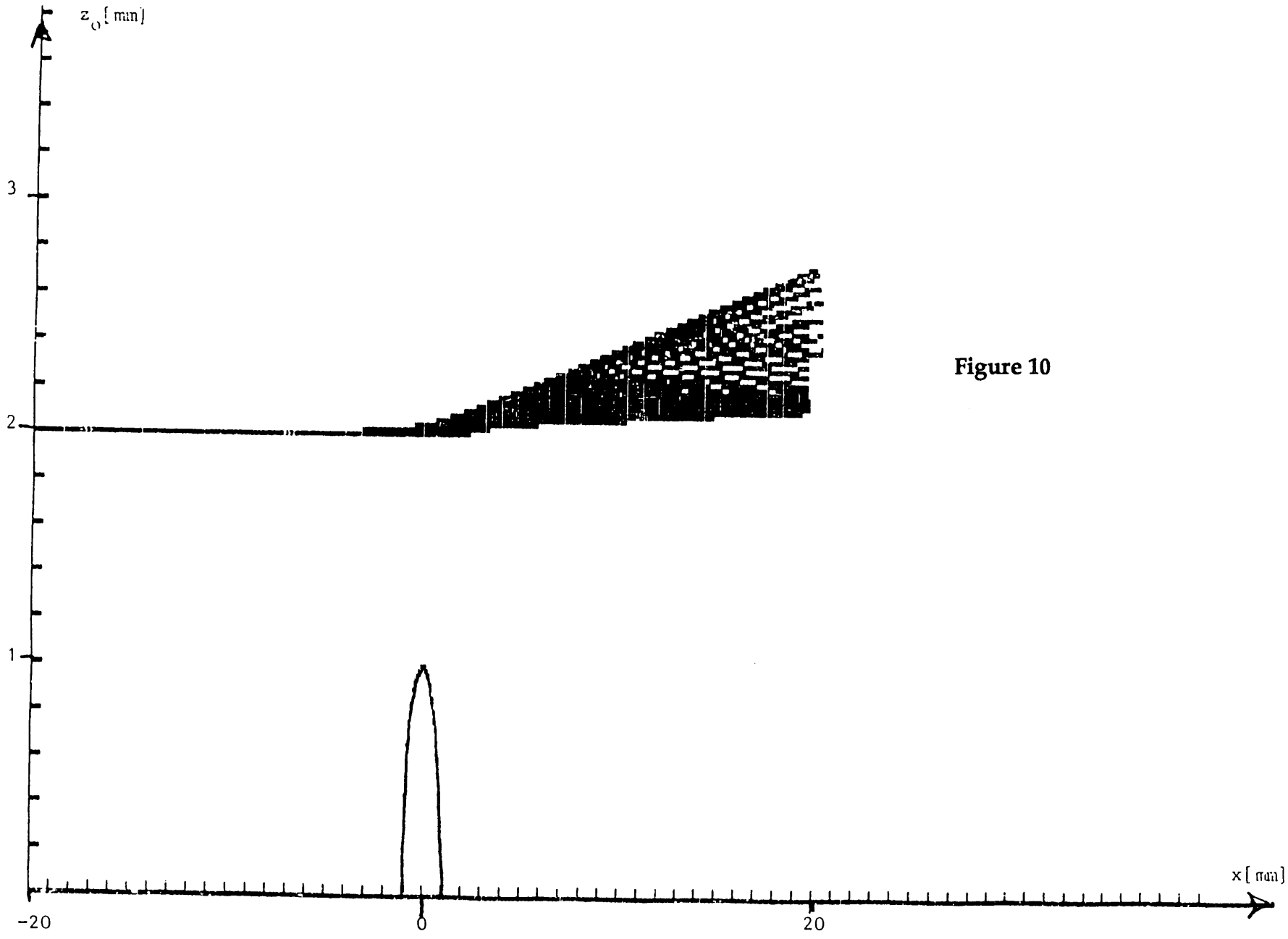

Figure 10

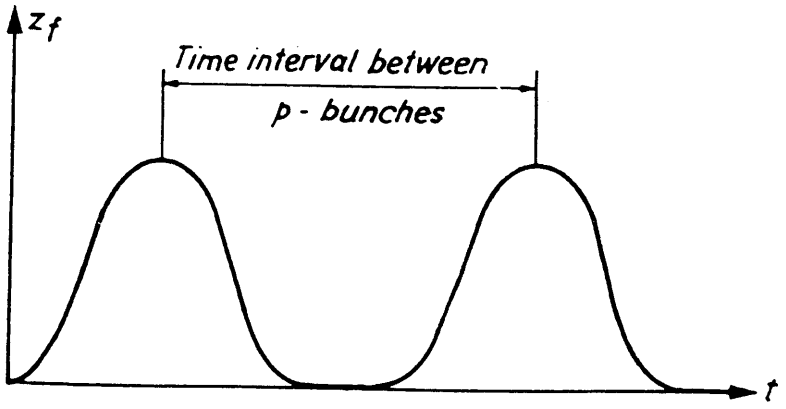

Figure 11

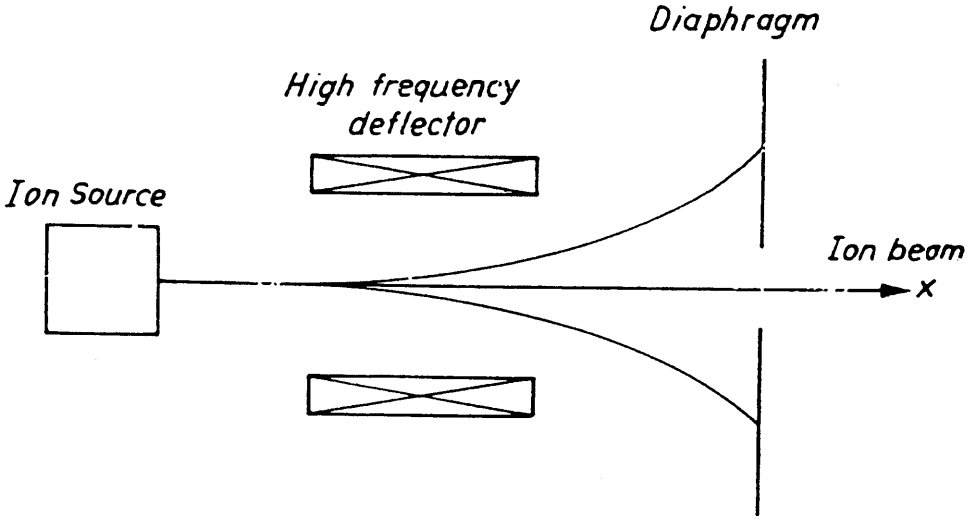

Figure 12

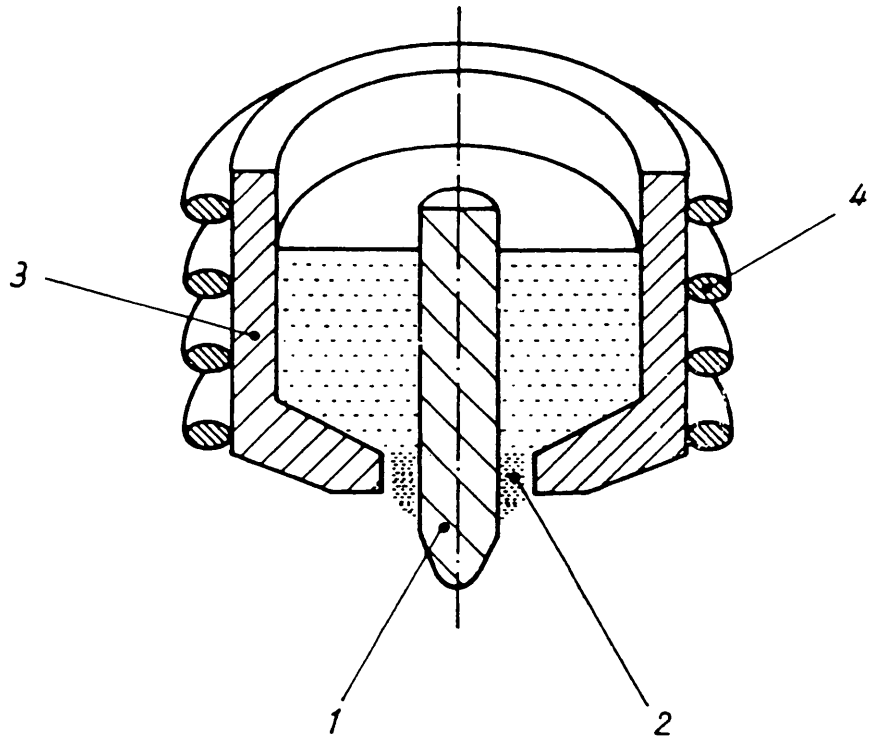

Figure 13

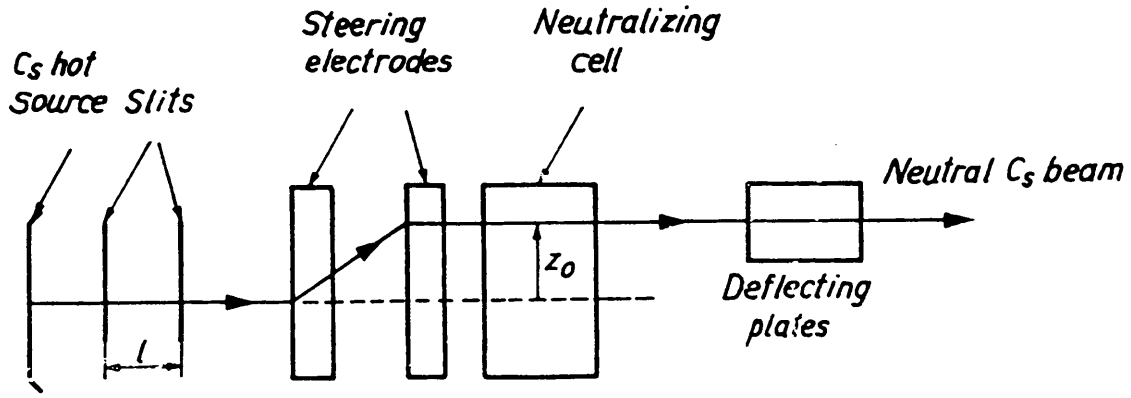

Figure 14

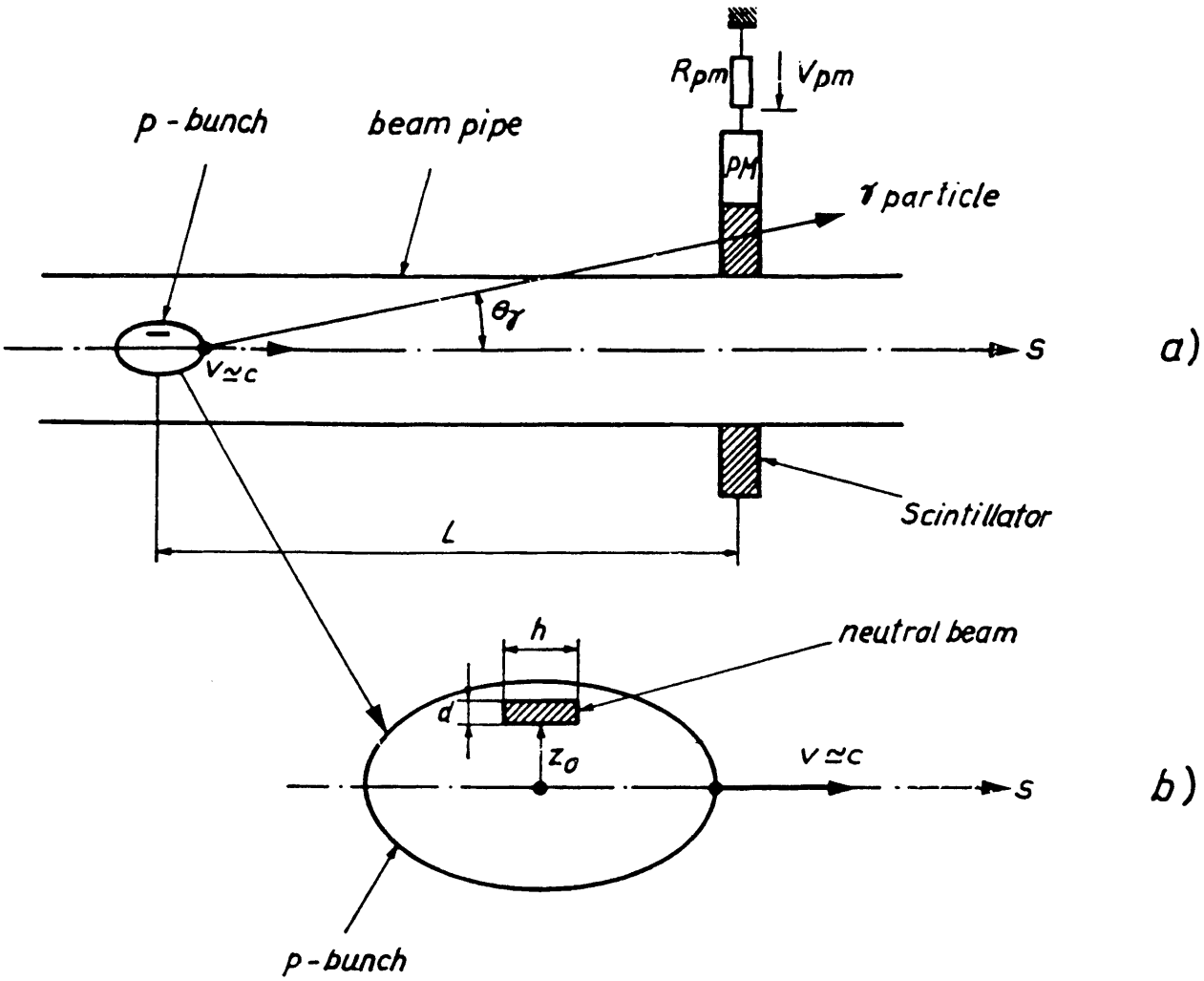
Rpm
Vpm
p - bunch
beam pipe
PM
γ particle
θγ
V≃c
s
a)
Scintillator
L
h
neutral beam
d
z0
V≃c
s
b)
p - bunch

Figure 15

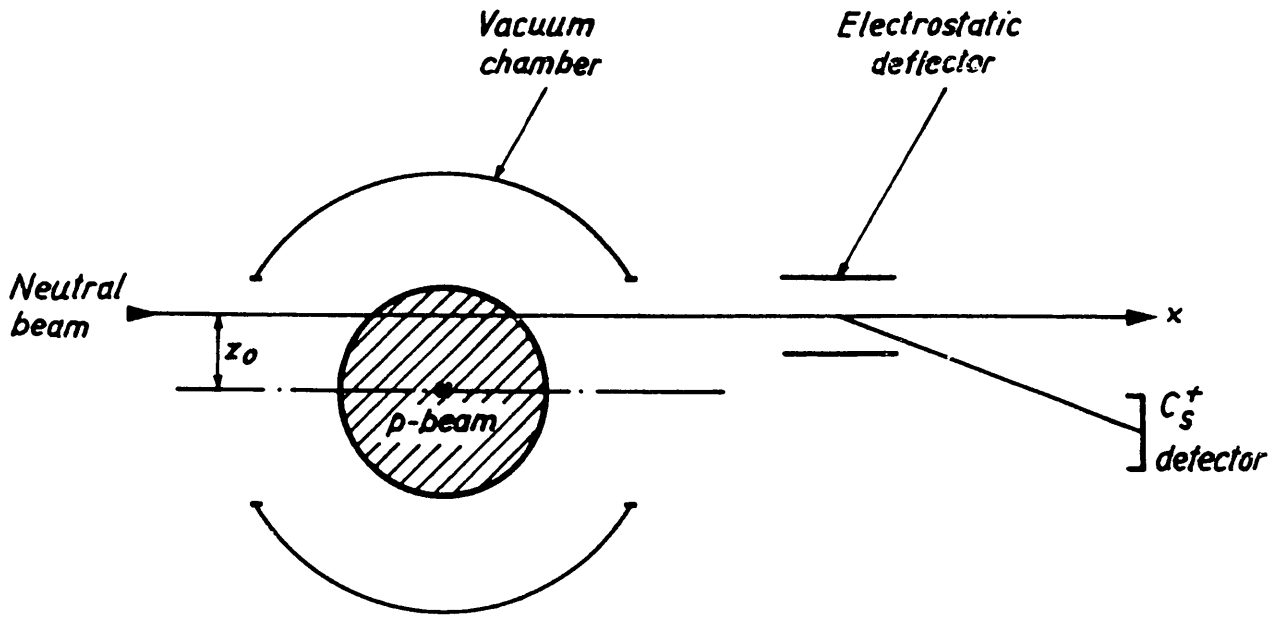
Vacuum
chamber
Electrostatic
deflector
Neutral
beam
z_o
p-beam
x
C_s^+
detector

Figure 16

t_0[s]	θ[rad]
t0= 2.23E-08	,theta= 2.00E-02
t0= 2.20E-08	,theta= 2.32E-02
t0= 2.17E-08	,theta= 2.66E-02
t0= 2.14E-08	,theta= 3.01E-02
t0= 2.11E-08	,theta= 3.31E-02
t0= 2.08E-08	,theta= 3.53E-02
t0= 2.04E-08	,theta= 3.62E-02
t0= 2.01E-08	,theta= 3.57E-02
t0= 1.98E-08	,theta= 3.39E-02
t0= 1.95E-08	,theta= 3.10E-02
t0= 1.92E-08	,theta= 2.76E-02
t0= 1.89E-08	,theta= 2.41E-02
t0= 1.86E-08	,theta= 2.08E-02
t0= 1.83E-08	,theta= 1.79E-02
t0= 1.79E-08	,theta= 1.54E-02
t0= 1.76E-08	,theta= 1.33E-02
t0= 1.73E-08	,theta= 1.15E-02
t0= 1.70E-08	,theta= 1.00E-02
t0= 1.67E-08	,theta= 8.77E-03
t0= 1.64E-08	,theta= 7.73E-03
t0= 1.61E-08	,theta= 6.84E-03
t0= 1.57E-08	,theta= 6.09E-03
t0= 1.54E-08	,theta= 5.46E-03
t0= 1.51E-08	,theta= 4.91E-03
t0= 1.48E-08	,theta= 4.44E-03

Table 3.1

z_o[m]	θ_m[rad]
z0= 2.00E-03	,thetmx= 3.62E-02
z0= 1.80E-03	,thetmx= 3.93E-02
z0= 1.60E-03	,thetmx= 4.24E-02
z0= 1.40E-03	,thetmx= 4.50E-02
z0= 1.20E-03	,thetmx= 4.66E-02
z0= 1.00E-03	,thetmx= 4.63E-02
z0= 8.00E-04	,thetmx= 4.33E-02
z0= 6.00E-04	,thetmx= 3.70E-02
z0= 4.00E-04	,thetmx= 2.71E-02
z0= 2.00E-04	,thetmx= 1.44E-02

Table 3.2